International Journal of Information, Control and Computer Sciences
ISSN: 2517-9942
Vol:6, No:7, 2012

Detecting Subsurface Circular Objects from Low Contrast Noisy Images: Applications in Microscope Image Enhancement

Soham De, *Member, IEEE,* Nupur Biswas, Abhijit Sanyal, Pulak Ray and Alokmay Datta

***Abstract*—**Particle detection in very noisy and low contrast images is an active field of research in image processing. In this article, a method is proposed for the efficient detection and sizing of subsurface spherical particles, which is used for the processing of softly fused Au nanoparticles. Transmission Electron Microscopy is used for imaging the nanoparticles, and the proposed algorithm has been tested with the two-dimensional projected TEM images obtained. Results are compared with the data obtained by transmission optical spectroscopy, as well as with conventional circular object detection algorithms.

***Keywords*—**Transmission Electron Microscopy, Circular Hough Transform, Au Nanoparticles, Median Filter, Laplacian Sharpening Filter, Canny Edge Detection

I. Introduction

PARTICLE detection and size determination in noisy and low contrast images is a challenging problem in image processing [1]. Noise and low contrast are more significant problems encountered while imaging particles which are subsurface in nature. In this article, a method is proposed for the efficient detection and size determination of subsurface spherical particles, which is used for the processing of softly fused Au nanoparticles.

There are two main sources of problems regarding shape detection from real images – due to the imaging technique, and due to problems in the shape inconsistency of the sample itself. In this implementation we are primarily dealing with a problem of the second category with of course the co-existence of the problem of the first category.

Here we have Transmission Electron Microscopy (TEM) images in real space of objects that are 'softly' fused, i.e. hard objects connected by soft gluey 'strips' - Au nanoparticles (NPs) connected through organic coatings or cappings that can attach to multiple nanoparticles. Nanoparticles are interesting fundamentally because they have size and shape dependant properties. All properties become uniquely defined only when the size and/or shape become well-defined, i.e. fall predominantly within a range for a collection of nanoparticles, known as shape/size 'monodispersity'. It is particularly to be noted that ultra-high resolution images of the atomic lattices within the NPs are not strictly relevant here, as overall and interfacial morphology of the particles, rather than their lattice, determine the properties. Hence detection and accurate measurement of shape and size of the nanoparticles is of crucial importance. This aspect underscores the relevance of this work.

Notwithstanding the fact that TEM provides most well-resolved images, there are certain limitations of imaging the NPs using TEM. Using electrons for subsurface imaging lead to problems as they are affected by the sample's chemical content. This leads to non-uniform illumination of the sample, and finally leading to high noise and weak edges in the TEM images produced. Thus an efficient algorithm is essential for detection and sizing of the nanoparticles in the TEM images.

The Circular Hough Transform (CHT) [2], an extension of the General Hough Transform [3], is the most popular method for circle detection in images. The principle of a Hough Transform is the transformation of the image to a parameter space, called the Hough space. The CHT is expected and has been previously shown to work well with noisy images, however it is inefficient in detecting nanoparticles from the micrographs due to excessive noise. Thus a modification to the CHT has been proposed in this article. For more efficient noise reduction, some preprocessing of the images is also proposed.

There has been some prior work on nanoparticle detection from TEM images. Woehrle et al [4] discusses how certain image processing software can be used for counting the number of nanoparticles present in a TEM image. However the method fails for samples which contain varying nanoparticle sizes in them. Fisker et al [5] proposes a deformable ellipse model for the detection and size determination. However, the method is inefficient for irregular particle size, as well as overlapped particles. It is also a very computationally expensive method. There have been some other work in particle detection from electron micrographs in the past [6], [7], [8], [9], [10], however, the level of false positives remains very high. Thus there is a need for a faster, and more efficient automatic image analysis method for the detection and sizing of nanoparticles.

In this article, a 3-step algorithm is proposed for the efficient detection and sizing of the NPs from the TEM images. The first step was to attempt to decrease the noise while making sure that the edges are not blurred. For this, we use the Median Filter [7] alongwith the Laplacian Sharpening Filter [7].

In the second step, for edge detection, we used the Canny edge detector [11]. This is used instead of the Sobel edge detector, as it shows better performance in detecting thin as well as low contrast edges.

To construct an efficient algorithm for the detection of

Soham De is with the Department of Computer Science & Engineering, Jadavpur University, Kolkata, India. e-mail: sohamde@ieee.org
Nupur Biswas, Abhijit Sanyal and Alokmay Datta are with the Applied Material Science Division, Saha Institute of Nuclear Physics, Kolkata, India.
Pulak Ray is with the Biophysics Division, Saha Institute of Nuclear Physics, Kolkata, India.

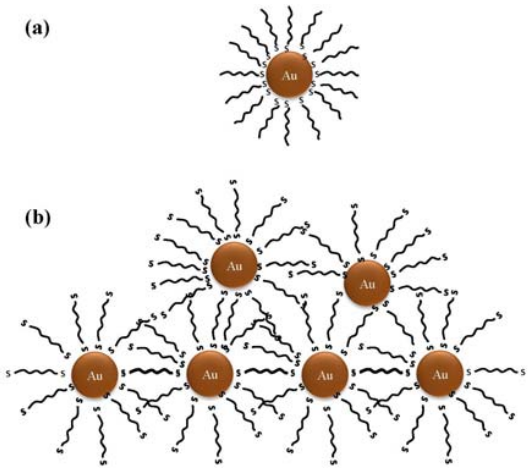

Fig. 1. Schematic of (a) Thiol-capped Au nanoparticle, (b) dithiol-capped Au nanoparticles

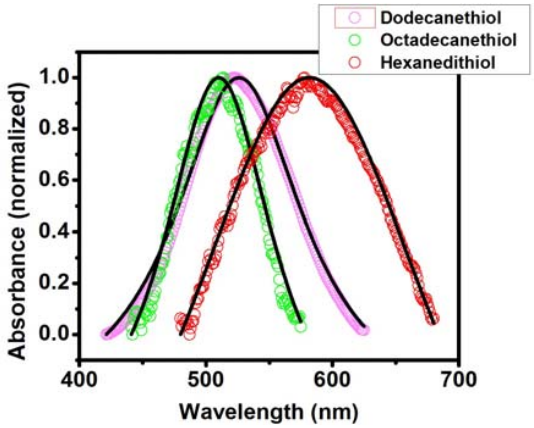

Fig. 2. Surface Plasmon Resonance (SPR) peaks of Au nanoparticles with different cappings. Black lines correspond to Lorentzian fit, while open circles represent the data for dodecanethiol (magenta), octadecaethiol (orange) and hexanedithiol (green) -capped NPs.

nanoparticles in an image, as much possible prior information should be incorporated into the algorithm. In the growth technique employed, it is expected that the NPs would be spherical, so circular patterns in a 2D projection are of main interest. Thus for the final step, we employed a modified version of the Circular Hough Transform for more efficient detection and extraction of the particles. The modifications take into account the low contrast nature of the images. In addition, the TEM images obtained do not yield perfectly circular projections of the spherical nanoparticles as the Au nanoparticles are interconnected through organic coatings. Thus our modified CHT takes into account this object irregularity and the corresponding uncertainty in radii.

Since this is not an online implementation, priority is given on accuracy than on time complexity. However, the Circular Hough Transform is very easy to highly parallelize when implemented in hardware, thus leading to very fast execution.

This paper is organized as follows. Section 2 investigates the methodology used in our research. In Section 3, we report the results obtained on imaging the nanoparticles. We also discuss the pitfalls of the algorithm. Final conclusions are presented in Section 4.

II. Experiments & Methodology

A. Preparation of Au nanoparticles with different cappings.

Preparation of Au nanoparticles of different cappings were primarily based on the widely used Brust-Schiffrin (BS) two-phase synthetic method [12]. We have prepared Au nanoparticles with three types of capping. In each case, Au was extracted from aqueous solution of $HAuCl_4$ by transferring it to an organic solution of toluene by using a phase transfer reagent TOABr (tetraoctylammonium bromide). After that the capping agent (dodecanethiol ($C_{12}H_{25}SH$), octadecanethiol ($C_{18}H_{37}SH$) or 1,6-hexanedithiol ($C_6H_{12}(SH)_2$)) is added to this phase separated solution and finally $HAuCl_4$ is reduced using aqueous solution of sodium borohydride ($NaBH_4$). The capped Au nanoparticles precipitate in ethanol solution when left overnight. This precipitate is washed with ethanol, filtered, and the residue on the filter paper is dissolved in toluene according to the desired concentration. It is to be mentioned that the S atom of the thiol chain attaches to the Au atoms of the core of nanoparticles to make them stable (Fig. 1). Among the cappings, the dithiol, due to the existence of S atoms at both ends of the carbon chain, can bind to two Au nanoparticles and is capable of producing a self-assembled string of superclusters [13] as shown in the cartoon of Fig. 1(b).

All chemicals were bought from Sigma-Aldrich, USA and used without further purification.

B. UV-Vis Spectroscopy

As an independent assessment of the sizes of these variously capped nanoparticles, we carried out transmission optical spectroscopy to investigate the surface plasmon resonance (SPR) bands of these nanoparticles using a GBC Cintra 10e UV-Vis spectrometer. The average size (d) of the nanoparticles is related to the FWHM (Γ) of the SPR band through the relation $d = \frac{2v_F}{\Gamma}$ where v_F is the Fermi velocity of the Au [14]. The SPR bands in question are shown in Fig. 2. It should be noted that while the SPR band for dodecanethiol-capped nanoparticles is very well fit by a Lorentzian, both octadecanethiol-capped and hexanedithiol-capped Au NP bands show small deviations from Lorentzian distributions. Nevertheless, as the deviations are small the FWHMs can give reliable estimate of NP sizes. Thiol-capped Au nanoparticles show no shift in the SPR peak ($526nm$ for dodecanethiol, $510nm$ for octadecanethiol) whereas the dithiol-capped nanoparticles show a red-shift ($568nm$) probably due to the denser coating with higher dipole moment that gives rise to a higher dielectric constant [15]. From SPR, the size of the metallic nanoparticles core come out to be $3.5nm$, $3.4nm$, $2.6nm$ for dodecanethiol, octadecanethiol and hexanedithiol respectively.

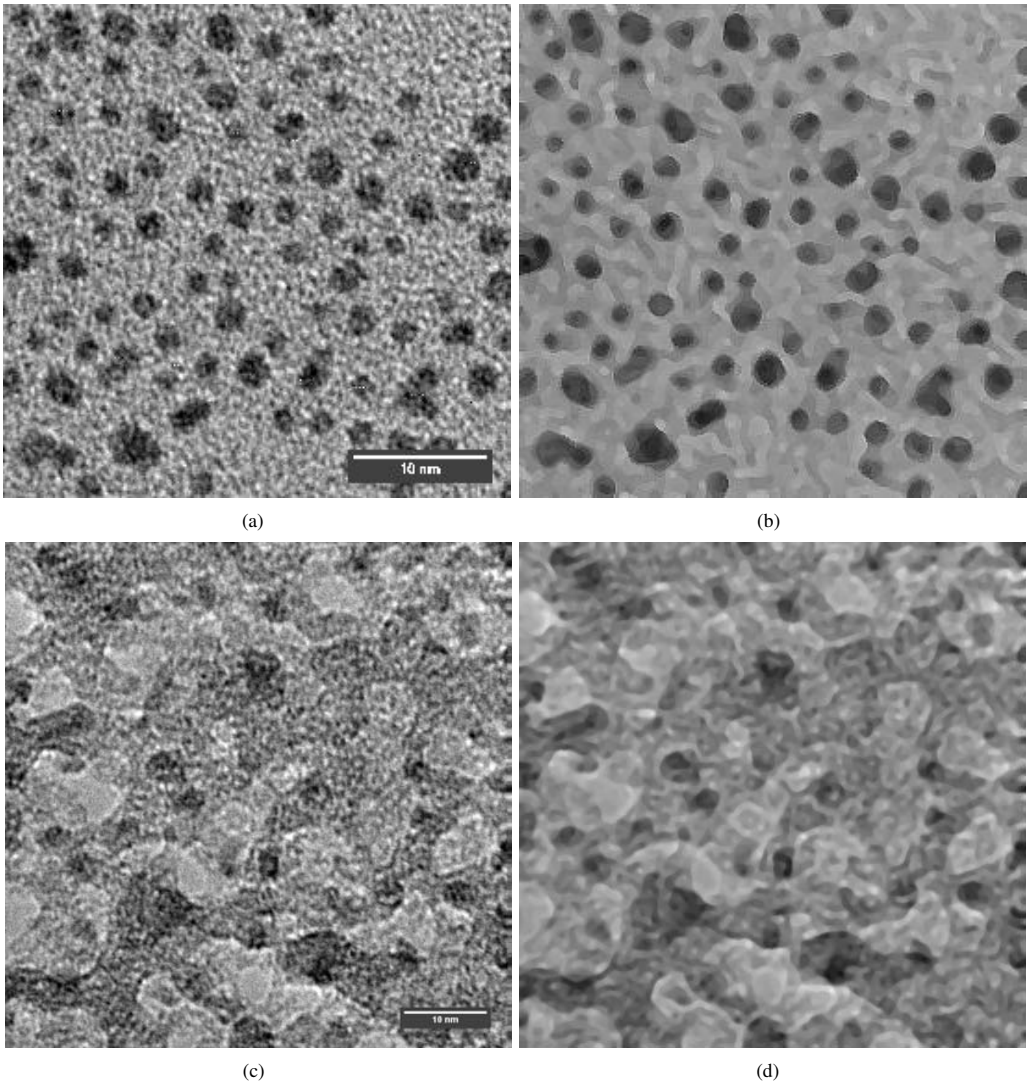

Fig. 3. Effect of pre-processing with the Median Filter and the Laplacian Sharpening Filter on the original TEM images. Original images are shown in (a) (Dodecanethiol-capped Au NPs) and (c) (Hexanedithiol-capped Au NPs), while the pre-processed images are shown in (b) and (d) respectively.

C. Transmission Electron Microscopy

To probe these nanoparticles by TEM we have used carbon-coated copper grid containing around 400 square meshes. Few microlitres of nanoparticle solution in toluene were drop-cast on the grid which was kept over a Whatman Grade 1, $150mm$ diameter filter paper with particle retention capacity 11 micron in liquid. The excess solvent trickled to the filter paper underneath and dried out completely within an overnight, in a desiccator.

TEM images were taken using a FEI electron microscope of model Technai S-twin, operating at accelerating voltage $200kV$ with a resolution of $2.4\mathring{A}$. TEM images were analyzed using ImageJ software (National Institute of Health, USA). It is to be noted that both TEM and SPR provide the size of the diameter of the metal core only.

Well-resolved nanoparticle images were obtained for the thiol-capped Au nanoparticles as shown in Fig. 5(a) and (b) for dodecanethiol and octadecanethiol-capped nanoparticles, respectively. However, for dithiol-capped nanoparticles the images (Fig. 5(c)) were unresolvable a priori, and to the end of resolving the shapes and sizes of these particles, the methods described in the succeeding sections have been employed.

D. Pre-processing Performed on the TEM Images

The TEM images obtained contained very noisy backgrounds and some pre-processing was required for reducing the noise in the images. We used a two step process for this. We first used the Median Filter, and then the Laplacian Sharpening Filter. The effect of using these filters together is shown in Fig. 3. Fig. 3(a) and 3(c) are two TEM images obtained from the dodecanthiol and hexanedithiol-capped nanoparticles respectively. We find, particularly in case of Fig. 3(c), that the

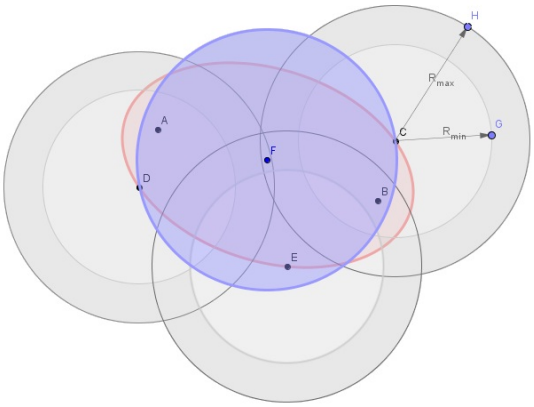

Fig. 4. The Modified Circular Hough Transform Explained. The red ellipse denotes the particle with A and B as foci. C, D and E are some of the points on the particle (ellipse) which vote for a radii range (R_{min} to R_{max}). From our algorithm, we get F as the center of the detected blue circle.

nanoparticles are not determinable even by the naked eye. But after using the Median Filter and the Laplacian Sharpening Filter, the image were better resolved and could be used for further processing as shown in Fig. 3(b) and 3(d).

'Salt and pepper' noise or impulse noise was removed by applying the Median Filter. Impulse points are those that have an absolutely different colour from their neighbouring pixels. The Median Filter replaces the value of a noise pixel with the median gray levels in the neighbourhood of that pixel. Thus it removes the impulse noise present in the image, but an extra consequence is the blurring of the edges. To take care of this we used the Laplacian Sharpening Filter as the second step of the pre-processing.

The purpose of using this filter is for highlighting fine details and enhancing those which are blurred such as edges. The Laplacian is a 2D isotropic measure of the 2^{nd} spatial derivative of an image. It highlights regions of rapid intensity change and is thus very effective in enhancing blurred edges.

Since the input image is represented as a set of discrete pixels, we have to find a discrete convolution kernel that can approximate the second derivatives in the definition of the Laplacian. We use the following kernel.

$$A = \begin{pmatrix} -1 & -1 & -1 \\ -1 & 8 & -1 \\ -1 & -1 & -1 \end{pmatrix}$$

The kernel approximates a second derivative measurement on the image, and is thus very sensitive to noise. This results in an increase in noise in the image. However using it with the median filter avoids this problem from occurring.

In all implementations of filters in the proposed algorithm, we used the classical implementation of convolution. Inventing input pixel values for places where the kernel extends off the end of the image has been avoided as it can lead to the distortion of the output image.

E. Canny Edge Detection

In general, the purpose of edge detection is to significantly reduce the amount of data in an image, while preserving the structural properties to be used for further image processing. There are various edge detecting algorithms, but in this algorithm we used Canny edge detection, as it shows better performance in detecting thin edges as well as low contrast edges.

The Canny edge detection algorithm used was as follows:

- *Gaussian Smoothing*: After applying the Laplacian Sharpening Filter, the image contained some noise and is thus first smoothened by applying a Gaussian filter. This step smoothens small noises in contrast to the Median Filter that causes impulse noise to reduce.We used a small standard deviation and a $3 * 3$ kernel to reduce the small noise incorporated into the image by the Laplacian Filter.
- *Gradient Calculation*: The gradient magnitude and direction of each pixel of the image was determined by the Sobel operator.
- *Non-maximum suppression*: This step converted the blurred edges in the image of the gradient magnitudes to sharp edges by preserving all local maxima in the gradient image, and deleting everything else.
- *Double thresholding and hysteresis*: Pixels stronger than the high threshold were considered edges, those weaker than the low threshold were considered as background and those between the two thresholds were marked as weak edges. Weak edges were included in the image if and only if they were connected to strong edges.

F. Modified Circular Hough Transform

The Hough Transform (HT) has been recognized as a very powerful tool for the detection of parametric curves in images. It implements a voting process that maps image edge points into manifolds in an appropriately defined parameter space. Peaks in the space correspond to the parameters of detected curves. The Circular Hough Transform (CHT) is designed to find a circle characterized by a center point (x_0, y_0) and a radius r. The CHT is computationally more expensive than line detection algorithms, due to the greater number of parameters involved. To determine a circle, it is necessary to accumulate votes in the three-dimensional parameter space (x_0, y_0, r). We limited the time required for the circle detection in our algorithm by incorporating a rough range that the NPs are expected to fall in.

As shown in Figs. 5(a), (b), (c), the TEM images of the nanoparticles have very noisy backgrounds, with low contrast making their detection harder. Moreover, the particles do not show up as perfectly circular and have a distorted shape. This is because the Au NPs are connected through organic coatings. Thus the Circular Hough Transform needs to be made more robust considering this object irregularity, and the corresponding uncertainty in radius [16].

For dealing with this problem, we let each point in the image space vote for a radius range in the parameter space, rather than for a single point. The radius range corresponds to the uncertainty in radius of the nanoparticle.

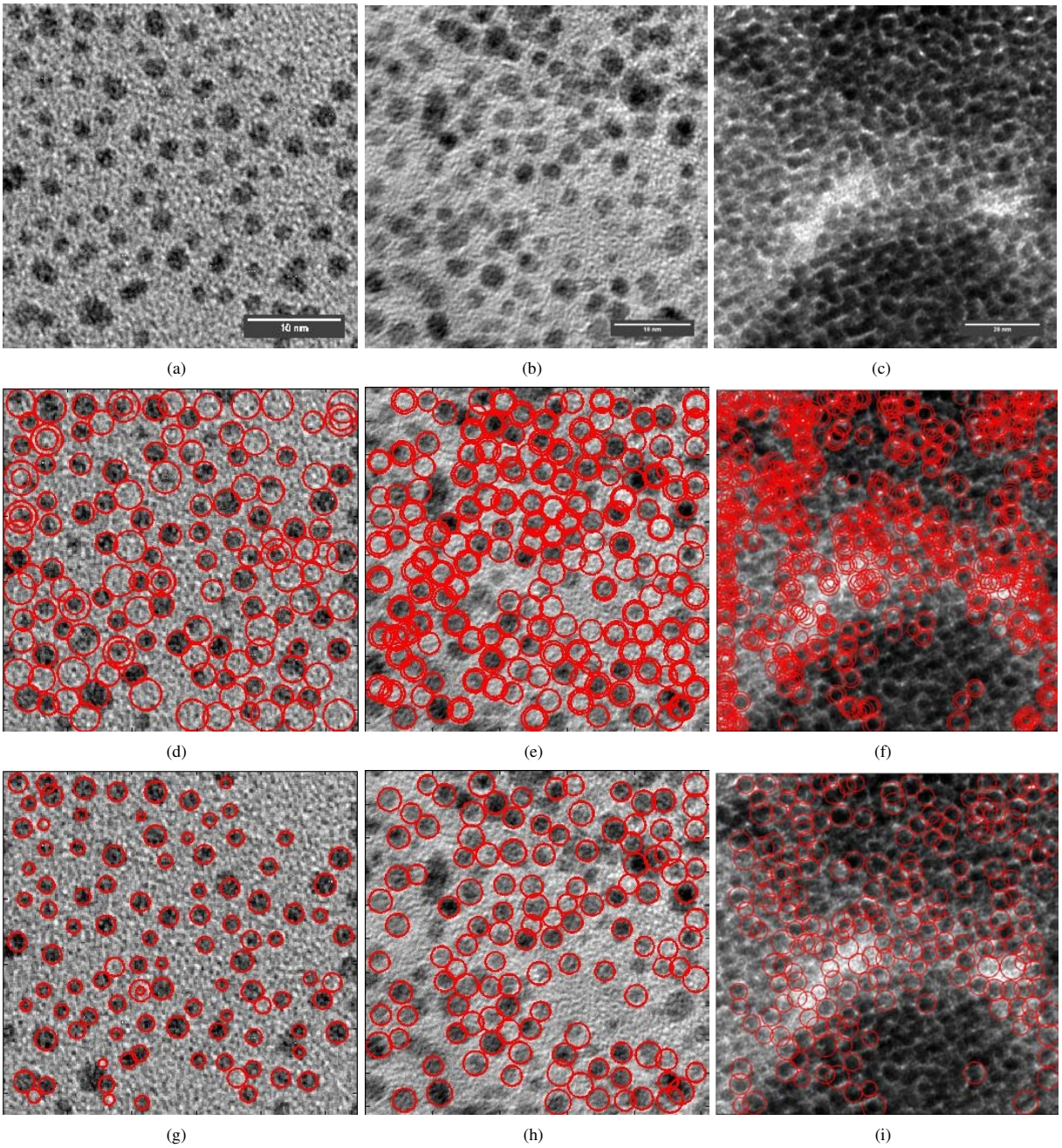

Fig. 5. Effect of Canny Edge Detection and Circular Hough Transform after the proposed pre-processing. Original TEM images of (a) dodecanethiol, (b) octadecanethiol (c) and hexanedithiol capped Au NPs; Images after application of Canny Edge Detector and CHT without any pre-processing shown in (d), (e), (f) and after application of Canny Edge Detection and the Modified CHT shown in (g), (h), (i), respectively. NPs detected by both schema are shown by red circles.

Since there were multiple nanoparticles in each image, there would be multiple peaks in the accumulator array. Thus we face the next problem of identifying those smaller peaks which were near another peak and were the result of the same particle, and thus needed to be ignored for correct computation. We implemented the following algorithm for taking care of this problem.

Once we got a peak in the accumulator array, we discarded all peaks which were smaller than the original peak and which lay within the Manhattan Distance of $2xr_{min}$ around the peak. If we found a peak of higher value, we took this as the new peak, and discarded the previously considered peak. The radius of the particle was taken to be a simple average of all the radii of all the points voting for that point, as present in the

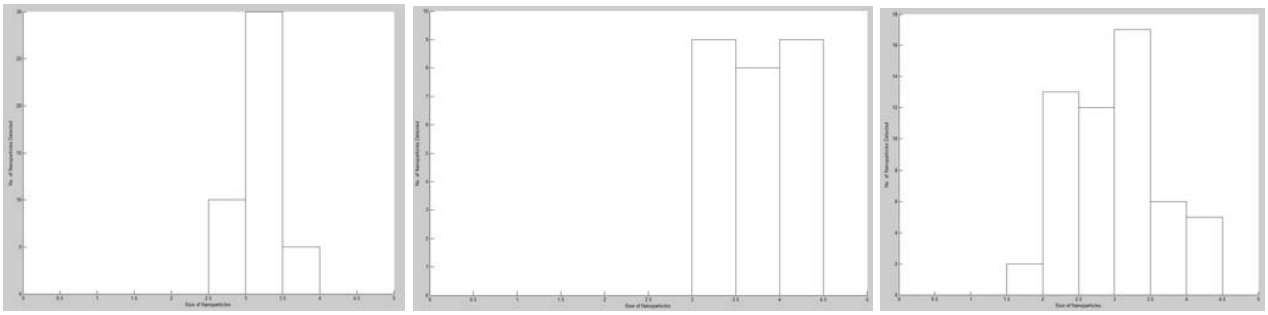

(a) (b) (c)

Fig. 6. Histograms of the distributions of NP sizes as obtained from Fig. 5(g), (h), (i) respectively for Au NPs capped with (a) dodecanethiol, (b) octadecanethiol, and (c) hexanedithiol. The x-axis denotes the size of the nanoparticles in nm, and the y-axis denotes the number of objects detected in the TEM images.

accumulator array.

$$R = \frac{1}{n}\sum_{i=1}^{n} R_i \tag{1}$$

This simple algorithm effectively approximated the nanoparticles as circles and we were able to determine the size of the NPs.

The algorithm is explained in Fig. 4. The red ellipse denotes the particle with A and B as foci. C, D and E are some of the points on the particle (ellipse) which vote for a radii range (R_{min} to R_{max}). From our algorithm, we get F as the center of the detected blue circle. Thus we see that this algorithm efficiently approximates an irregular shaped particle.

III. Results

The proposed shape detection algorithm was tested with Au nanoparticles of all three types of cappings. A total of 2, 14 and 18 images were taken of the Au nanoparticles with capping agents dodecanethiol, octadecanethiol and 1,6-hexanedithiol, respectively.

Figs. 5(a),(b),(c) show one original TEM image obtained of the Au nanoparticles for the each of the respective capping agents. As is evident, the images are very noisy with low contrast, especially for the hexanedithiol-capped particles.

Figs. 5(d),(e),(f) show the detected particles using the conventional implementation of the Canny edge detector, and the Circular Hough Transform. The contours of the detected objects are shown by red circles in the figures. The conventional method does not efficiently detect the nanoparticles, and detects many false particles as shown.

Figs. 5(g),(h),(i) show the detected objects in the images using our proposed algorithm. We see that the octadecanethiol and dodecanethiol-capped Au nanoparticles are all detected successfully in the images. The 1,6-hexanedithiol-capped images are slightly less resolvable than these, but the resolution shows considerable improvement over Fig. 5(f).

Figs. 6(a),(b),(c) show the radii distributions for the particles in nanometer scale in each of the three cases. From the distributions we see that the sizes of the metallic nanoparticle core comes out to be $3.3nm$, $3.6nm$ and $2.9nm$ for dodecanethiol, octadecanethiol and hexanedithiol respectively. This compares well to the SPR data obtained, as mentioned before, of sizes $3.5nm, 3.4nm$ and $2.6nm$, in the three cases in the same order.

What is more remarkable is that the size distribution of the dodecanethiol-capped Au NPs is consistent with the Lorentzian distribution of the same as obtained from the SPR data, while those of octadecanethiol, and hexanedithiol-capped NPs deviate considerably from log-normal behaviour, again showing consistency with deviations from Lorentzian behaviour in the corresponding SPR results.

IV. Conclusion

In this paper, we have proposed a method for efficient detection of circular objects from noisy low contrast 2-dimensional projected images of subsurface spherical objects. We tested our shape detection method for the detection and processing of Transmission Electron Micrographs of Au nanoparticles with three types of cappings, using capping agents as dodecanethiol, octadecanethiol and 1,6-hexanedithiol. The results obtained were compared with those of Surface Plasmon Resonance data, as well as with conventional image analysis methods, and were found to give good results.

The proposed method could have varied applications. Examples are the detection of submerged buildings during floods, or dynamic obstacle detection while moving through foggy areas. We plan to extend our study on these applications in the future.

Other than these, this work forms the first step in the implementation of on-line, real-time, on-chip image and data processing through a Field Programmable Gate Array (FPGA) that is capable of high speed operations and has a large embedded memory.

References

[1] William V Nicholson and Robert M Glaeser. Review: Automatic particle detection in electron microscopy. *Journal of Structural Biology*, 133(2/3):90–101, 2001.

[2] Richard O Duda and Peter E Hart. Use of the Hough transformation to detect lines and curves in pictures. *Communications of the ACM*, 15(1):11–15, 1972.

[3] Paul V C Hough. Method and means for recognizing complex patterns, 1962.

[4] G H Woehrle, J E Hutchison, S Ozkar, and R G Finke. Analysis of nanoparticle Transmission Electron Microscopy data using a public-domain image-processing program, Image. *Turkish Journal of Chemistry*, 30(1):1–13, 2006.
[5] R Fisker, J M Carstensen, M F Hansen, F Bø dker, and S Mø rup. Estimation of nanoparticle size distributions by image analysis. *Journal of Nanoparticle Research*, 2(3):267–277, 2000.
[6] A. Saad, W. Chiu, and P. Thuman-Commike. Multiresolution approach to automatic detection of spherical particles from electron cryomicroscopy images. In *ICIP 98. Proceedings. International Conference on Image Processing*, pages 846–850, 1998.
[7] Rafael C Gonzalez and Richard E Woods. *Digital Image Processing*, volume 49 of *Texts in Computer Science*. Prentice Hall, 2008.
[8] K R Lata, P Penczek, and J Frank. Automatic particle picking from electron micrographs. *Ultramicroscopy*, 58(3-4):381–391, 1995.
[9] G Harauz and A Fong-Lochovsky. Automatic selection of macromolecules from electron micrographs by component labelling and symbolic processing. *Ultramicroscopy*, 31(4):333–344, 1989.
[10] Dana H Ballard and Christopher M Brown. *Computer Vision*, volume Computer S. Prentice Hall, 1982.
[11] J Canny. A Computational Approach to Edge Detection. *IEEE Transactions on Pattern Analysis and Machine Intelligence*, 8(6):679–698, 1986.
[12] Mathias Brust, Merryl Walker, Donald Bethell, David J Schiffrin, and Robin Whyman. Synthesis of thiol-derivatised gold nanoparticles in a two-phase Liquid-Liquid system. *Journal of the Chemical Society Chemical Communications*, 1994(7):801, 1994.
[13] Mathias Brust, David J Schiffrin, Donald Bethell, and Christopher J Kiely. Novel gold-dithiol nano-networks with non-metallic electronic properties. *Advanced Materials*, 7(9):795–797, 1995.
[14] J Perenboom. Electronic properties of small metallic particles. *Physics Reports*, 78(2):173–292, 1981.
[15] Lorenza Suber. Permanent Magnetism in Dithiol-Capped Silver Nanoparticles. *Chemistry of Materials*, 19(6):1509–1517, 2007.
[16] Marcin Smereka and Ignacy Dulba. Circular Object Detection Using a Modified Hough Transform. *International Journal of Applied Mathematics and Computer Science*, 18(1):85–91, 2008.
[17] L A Bradshaw and J P Wikswo. Spatial filter approach for evaluation of the surface Laplacian of the electroencephalogram and magnetoencephalogram. *Annals of Biomedical Engineering*, 29(3):202–213, 2001.
[18] Nosrati Ali Nosrati Masoud, Karimi Ronak, Nosrati Hamed. A method for detection and extraction of circular shapes from noisy images using median filter and CHT. *Journal of American Science*, 7(6):84–88, 2011.
[19] B Schaffer, U Hohenester, A Trugler, and F Hofer. High-resolution surface plasmon imaging of gold nanoparticles by energy-filtered transmission electron microscopy. *Physical Review B*, 79(4):1–4, 2009.
[20] D H Ballard. Generalizing the Hough transform to detect arbitrary shapes. *Pattern Recognition*, 13(2):111–122, 1981.
[21] Olivier Le Bihan, Pierre Bonnafous, Laszlo Marak, Thomas Bickel, Sylvain Trépout, Stéphane Mornet, Felix De Haas, Hugues Talbot, Jean-Christophe Taveau, and Olivier Lambert. Cryo-electron tomography of nanoparticle transmigration into liposome. *Journal of Structural Biology*, 168(3):419–425, 2009.
[22] D Ioannou. Circle recognition through a 2D Hough Transform and radius histogramming. *Image and Vision Computing*, 17(1):15–26, 1999.
[23] Jingyue Liu. Scanning transmission electron microscopy and its application to the study of nanoparticles and nanoparticle systems. *Journal of Electron Microscopy*, 54(3):251–278, 2005.
[24] J Illingworth and J Kittler. A survey of the hough transform. *Computer Vision Graphics and Image Processing*, 44(1):87–116, 1988.
[25] Gonzalo R Arce. Nonlinear signal processing: a statistical approach. *Scientist*, 48(1):0,0, 2005.
[26] Carolyn Kimme, Dana Ballard, and Jack Sklansky. Finding circles by an array of accumulators. *Communications of the ACM*, 18(2):120–122, 1975.
[27] Z L Wang. Transmission Electron Microscopy of Shape-Controlled Nanocrystals and Their Assemblies. *The Journal of Physical Chemistry B*, 104(6):1153–1175, 2000.